PHYSICAL REVIEW B VOLUME 15, NUMBER 12 15 JUNE 1977

Theory of optical and microwave properties of microscopically inhomogeneous materials*

Itzhak Webman and Joshua Jortner
Department of Chemistry, Tel-Aviv University, Tel-Aviv, Israel

Morrel H. Cohen
The James Franck Institute and Department of Physics, The University of Chicago, Chicago, Illinois 60637

(Received 8 March 1976)

In this paper we present a theoretical study of the optical and microwave properties of microscopically inhomogeneous disordered materials. We derive an effective-medium theory (EMT) for the propagation of light in a heterogeneous system by means of a self-consistent extension of a multiple-scattering model. This approach is applicable when the correlation length for the fluctuation in the medium is much smaller than the optical wavelength. The Maxwell-Garnett theory is also shown to result from our model under less general circumstances. We present a scheme for the derivation of the macroscopic complex dielectric constant $\epsilon(\omega)$ through numerical simulations of the inhomogeneous medium, which can be viewed as a generalization of the numerical simulations of the electrical conductivity in resistor networks. On the basis of numerical simulations we assert that the EMT for $\epsilon(\omega)$ of a binary inhomogeneous medium is valid when the ratio $x(\omega)$ between the complex dielectric constants of the two components obeys the condition $0.05 < |x(\omega)| < 20$. Under more general conditions numerical simulations are more reliable than the EMT at the percolation transition region. The theory is applied to investigate the optical and microwave properties of some binary model systems. The results of this analysis are utilized to explain some optical and microwave properties of granular metallic films, metal-ammonia solutions, and amorphous germanium.

I. INTRODUCTION

The study of the optical properties of condensed systems with inhomogeneities small relative to the wavelength reveals anomalous phenomena that do not occur in the related homogeneous systems. Such phenomena, usually resonances in the optical conductivity, have been observed in aggregated metallic films,[1-4] in suspensions of fine metallic particles in a dielectric medium,[5-7] in colloidal color centers in alkali halide crystals,[8] and in amorphous germanium with voids.[9-11]

The behavior of some of these systems has been accounted for by means of the Maxwell-Garnett (MG) theory,[12-14] which is essentially a first-order multiple-scattering treatment for the propagation of an electromagnetic wave through a medium in which scatterers small relative to the wavelength λ are embedded. The MG theory is therefore appropriate for a binary composite material in which one of the components forms separate inclusions in a matrix formed by the other. In general, for random heterogeneous binary systems such a situation prevails only when the concentration of either component is smaller than the percolation threshold C^*.[15-18] For $C > C^*$ most of the volume of this component forms extended channels. There is evidence from numerical simulation of electronic transport in disordered systems[19-21] that for continuous percolation $C^* = 0.145 \pm 0.01$ while experimental data[22,23] indicate a value of C^* of 0.15–0.17. For such systems the MG theory is not appropriate in the region $C^* < C < 1 - C^*$.

In this work we present a self-consistent extension of the multiple-scattering model, which yields an effective-medium theory (EMT) for the propagation of light in a heterogeneous system. The effective-medium approximation for electronic transport properties[19,24-26] has been recently successfully applied to account for the behavior of some disordered materials which undergo metal-nonmetal transitions.[22,23,27,28] In those materials the transition takes place via an inhomogeneous regime in which percolation effects determine the transport properties. Concentrated metal-ammonia solutions have been studied extensively.[22] We have proposed that in the range of metal concentration 2.3–9 MPM (mole percent metal) Li-NH_3 and Na-NH_3 solutions consist of metallic and nonmetallic regions characterized by a short correlation length of 15–30 Å at ~10°K above the consolute temperature. Since this length is much smaller than the optical wavelength, one condition for the applicability of EMT to the optical constants is satisfied. The other condition for the validity of EMT is that fluctuations in the local microscopic values of the dielectric constant would not be too large. This condition is also met in metal-ammonia solutions.[29,30] Accordingly, we have presented elsewhere[31] an account of an analysis of the optical properties of metal-ammonia solutions based on EMT and the above inhomogeneous model.

The MG approximation has been used to explain the resonances that appear in systems composed of metallic clusters within a dielectric.[4,7,14] We find that in the limit of low metal concentration,

$C < 0.05$, the EMT reproduces the MG results, i.e., a Mie resonance at $\omega_R \cong \omega_p/(1+2\epsilon_0)^{1/2}$. However, as C increases beyond 0.1 the peak becomes very broad. We shall demonstrate that both the EMT and the MG formula correspond to special cases of a single-cell approximation for the frequency-dependent dielectric constant. The MG result is adequate for a binary system where one component is embedded as isolated regions in the other component, while the EMT constitutes a self-consistent approximation to the dielectric constant.

II. EFFECTIVE-MEDIUM APPROXIMATION FOR THE PROPAGATION OF LIGHT IN A RANDOM HETEROGENEOUS MEDIUM

We first review the effective medium theory for the static dielectric constant of a random heterogeneous medium, and then proceed to generalize the derivation for the optical case.

A random heterogeneous medium with correlation length b can be approximated by dividing its volume into cells of dimension b centered on the points $\vec{r}_1, \ldots, \vec{r}_N$ having a constant value of the dielectric constant ϵ_i in each cell i.

The assumption that the medium is random may be expressed by the fact that the N-cell distribution function $P(\epsilon_1, \ldots, \epsilon_N)$ is equal to the product of single-cell probability functions $P(\epsilon_1) \times P(\epsilon_2) \times P(\epsilon_N)$. The field and the displacement in the ith cell are evaluated assuming that the cell is embedded in a homogeneous medium of dielectric constant ϵ_0 and that the whole sample is in an external field $\vec{E}$. The effective dielectric constant is then defined as:

$$\epsilon(\epsilon_0) = \langle \vec{D}(\epsilon_i, \epsilon_0)\rangle / \langle \vec{E}(\epsilon_i, \epsilon_0)\rangle , \tag{2.1}$$

where $\langle f(\epsilon_i)\rangle$ stands for $\int P(\epsilon) f(\epsilon)\, d\epsilon$. This general single-cell approximation can be made self-consistent by setting $\epsilon(\epsilon_0) = \epsilon_0$. If the form of the cells is assumed to be spherical, Eq. (2.1) becomes

$$\epsilon = \epsilon_0 \left(1 + 2\left\langle \frac{\epsilon_i - \epsilon_0}{\epsilon_i + 2\epsilon_0}\right\rangle\right)\left(1 - \left\langle \frac{\epsilon_i - \epsilon_0}{\epsilon_i + 2\epsilon_0}\right\rangle\right)^{-1} . \tag{2.2}$$

Setting $\epsilon = \epsilon_0$ we get the EMT formula

$$\left\langle \frac{\epsilon_i - \epsilon}{\epsilon_i + 2\epsilon}\right\rangle = 0 . \tag{2.3}$$

For the case of binary system A, B in the limit of small concentration C_A of component A, one may set $\epsilon_0 = \epsilon_B$ and Eq. (2.2) becomes

$$\epsilon = \epsilon_B \left[1 + 2C_A\left(\frac{\epsilon_A - \epsilon_B}{\epsilon_A + 2\epsilon_B}\right)\right]\left[1 - C_A\left(\frac{\epsilon_A - \epsilon_B}{\epsilon_A + 2\epsilon_B}\right)\right]^{-1} . \tag{2.4}$$

It has been shown by Hashin and Strickman[32] that this expression and the expression obtained from Eq. (2.4) when B and A are exchanged constitute lower and the upper bounds, respectively (assuming $\epsilon_B < \epsilon_A$), for the exact value of the medium dielectric constant. However, this theorem is proved only for real ϵ or σ. Equation (2.3) for a binary system is symmetric in the two components. This does not apply to Eq. (2.4), which therefore is applicable only for small values of concentration of one component.

The above derivation of the EMT may be immediately generalized to the frequency-dependent case. ϵ_i is then complex and ω dependent. When the wavelength λ in the medium is much larger than the sample size, the sample can be said to be in a uniform average field, and the same arguments used for the static case hold. Springett has carried out such an analysis for the ac conductivity.[33]

In the more general case, λ smaller than sample size, one has to study the propagation of an electromagnetic wave through an inhomogeneous medium. We shall show that under the assumption that the correlation length b and the wavelength satisfy $b/\lambda \ll 1$, one still obtains formulas identical to Eqs. (2.2) and (2.3) for the complex dielectric constant. We make use of the Ewald-Oseen extinction theorem,[34] which is an integral equation for the wave propagating in a medium with scatterers. Within the single-cell approximation scheme we assume that the ith cell scatters as a spherical region of dielectric constant ϵ_i embedded in a medium of dielectric constant ϵ_0. The scattering amplitude under the condition $b \ll \lambda$ is proportional to the polarizability:

$$\alpha(\epsilon_i) = b^3(\epsilon_i - \epsilon_0)/(\epsilon_i + 2\epsilon_0) . \tag{2.5}$$

The integral for the propagation of a wave in the medium with given configuration of cells $\{\epsilon_1, \ldots, \epsilon_N\}$ is

$$\vec{E}(\vec{r}, \epsilon_1, \ldots, \epsilon_r, \ldots, \epsilon_N) = \vec{E}_0(\vec{r}) + \frac{3}{4\pi}\int_{S(\vec{r})}^{\Sigma} (\vec{\nabla}_{r'} \times \vec{\nabla}_{r'}) \times \alpha(\epsilon_{r'})\vec{E}(\vec{r}', \epsilon_1, \ldots, \epsilon_{r'}, \ldots, \epsilon_r, \ldots, \epsilon_N) G(|\vec{r} - \vec{r}'|)\, d\vec{r}' , \tag{2.6a}$$

where

$$G(|\vec{r} - \vec{r}'|) = e^{iK_0|\vec{r}-\vec{r}'|}/|\vec{r} - \vec{r}'| \tag{2.6b}$$

is the propagator for an assumed homogeneous medium of complex dielectric constant ϵ_0 where

$$k_0^2 = (\omega^2/C^2)\epsilon_0 ; \tag{2.7}$$

$\vec{E}_0(\vec{r})$ is an incident wave of wave vector k_0, which propagates in a homogeneous region of the medium characterized by a dielectric constant ϵ_0, and enters the inhomogeneous region via the boundary Σ between the two regions.

The integration is over all the volume of the inhomogeneous region excluding a sphere $S(\vec{r})$ of a size small relative to λ around the cell at $\vec{r}$. We proceed with the formal statistical arguments which lead to an equation for an averaged wave

$$\langle\vec{E}(\vec{r})\rangle^{(\epsilon_r)} = \vec{E}_0(\vec{r}) + \frac{3}{4\pi}\int_{S(\vec{r})}^{\Sigma} P(\epsilon_{r'})(\vec{\nabla}_{r'}\times\vec{\nabla}_{r'}) \times \alpha(\epsilon_{r'})\langle\vec{E}(\vec{r}')\rangle^{(\epsilon_r,\epsilon_{r'})} \times G(|\vec{r}-\vec{r}'|)\,d\vec{r}'\,d\epsilon_{r'}\,. \tag{2.8}$$

The average $\langle\ \rangle^{(\epsilon_r)}$ denotes the result of averaging over the configuration $\{\epsilon_1,\ldots,\epsilon_N\}$ excluding the cell at r. Here we introduce an approximation similar to the quasicrystalline approximation[35]:

$$\langle\vec{E}(\vec{r}')\rangle^{(\epsilon_r,\epsilon_{r'})} = \langle\vec{E}(\vec{r}')\rangle^{(\epsilon_{r'})}\,. \tag{2.9}$$

The physical content of this approximation is that the wave incident at $\vec{r}'$ does not depend on the content of the cell at $\vec{r}$.

Equation (2.8) can be viewed as the first equation in a hierarchy of averaged multiple-scattering equations, the next equation being an equation for $\langle E(r')\rangle^{(\epsilon_r,\epsilon_{r'})}$ and would have $\langle E(r'')\rangle^{(\epsilon_r,\epsilon_{r'},\epsilon_{r''})}$ in the integrand. Equation (2.9) is a procedure for the truncation of the hierarchy of equations.[36] Equation (2.8) can now be recast as[34]

$$\vec{Q}(\vec{r}) = \vec{E}_0(\vec{r}) + \frac{3}{4\pi}(\vec{\nabla}_r\times\vec{\nabla}_r)\times\int_{S(\vec{r})}^{\Sigma} P(\epsilon_{r'})\alpha(\epsilon_{r'})\vec{Q}(\vec{r}')G(|\vec{r}-\vec{r}'|)d\vec{r}'\,d\epsilon_{r'} - 2P(\epsilon_r)\alpha(\epsilon_r)\vec{Q}(\vec{r})\,, \tag{2.10a}$$

where

$$\vec{Q}(\vec{r}) = \langle\vec{E}(\vec{r})\rangle^{(\epsilon_r)}\,. \tag{2.10b}$$

The assumption represented by Eq. (2.9), together with the exclusion of the cell at r from the integral in Eq. (2.8), implies that $\langle E(r)\rangle^{(\epsilon_r)}$ does not depend on the content of the cell at r. We may therefore transform Eq. (2.10a) by averaging over $\epsilon_{r'}$ and ϵ_r into

$$\vec{Q}(\vec{r}) = \vec{E}_0(\vec{r}) + \frac{3}{4\pi}\langle\alpha\rangle(\vec{\nabla}_r\times\vec{\nabla}_r)\times\int_{S(\vec{r})}^{\Sigma}\vec{Q}(\vec{r}')G(|\vec{r}-\vec{r}'|)\,d\vec{r}' - 2\langle\alpha\rangle\vec{Q}(\vec{r})\,. \tag{2.11}$$

For a wave $\vec{Q}(r)$ which obeys the equation

$$\nabla^2\vec{Q}(\vec{r}) - k^2\vec{Q}(\vec{r}) = 0 \tag{2.12a}$$

with

$$k^2 = (\omega^2/C^2)\epsilon \tag{2.12b}$$

Eq. (2.11) reduces to[34]

$$\vec{Q}(\vec{r}) = \vec{E}_0(\vec{r}) + I_0(\vec{r}) + \langle\alpha\rangle\frac{3\epsilon}{\epsilon-\epsilon_0}\vec{Q}(\vec{r}) - 2\langle\alpha\rangle\vec{Q}(\vec{r})\,. \tag{2.13}$$

The term $I_0(r)$, which originates from the contribution of the surface Σ to the integral in Eq. (2.11), represents a wave propagating with a wave vector k_0 given by Eq. (2.7). Since $Q(r)$ propagates with a wave vector $k\neq k_0$ the term $\vec{E}_0(\vec{r})+I_0(\vec{r})$ vanishes inside the inhomogeneous medium. We are now left with the following equation for $\epsilon(\omega)$

$$[\epsilon(\omega)-\epsilon_0(\omega)]/[2\epsilon_0(\omega)+\epsilon(\omega)] = \langle\alpha(\omega)\rangle\,, \tag{2.14}$$

where $\langle\alpha(\omega)\rangle$ is the average polarizability of a region of statistically distributed $\epsilon_i(\omega)$ in a medium of dielectric constant $\epsilon_0(\omega)$. Solving for $\epsilon(\omega)$ using Eq. (2.5) we get an equation analogous to Eq. (2.2)

$$\epsilon(\omega) = \epsilon_0(\omega)\left(1 + 2\left\langle\frac{\epsilon_i(\omega)-\epsilon_0(\omega)}{\epsilon_i(\omega)+2\epsilon_0(\omega)}\right\rangle\right) \times\left(1 - \left\langle\frac{\epsilon_i(\omega)-\epsilon_0(\omega)}{\epsilon_i(\omega)+2\epsilon_0(\omega)}\right\rangle\right)^{-1} \tag{2.15}$$

and related to the Lorentz-Lorenz formula.[37] We can regard this formula as a single-cell approximation for $\epsilon(\omega)$, where $\epsilon_0(\omega)$ is any assumed initial homogeneous approximation for the medium.

For a binary system in the case when one component is embedded as isolated regions in the other component, it is reasonable to choose $\epsilon_0(\omega)$ equal to the dielectric constant of the matrix component, resulting in the Maxwell-Garnett formula,

$$\epsilon(\omega) = \epsilon_B(\omega)\left[1 + 2C_A\left(\frac{\epsilon_A(\omega)-\epsilon_B(\omega)}{\epsilon_A(\omega)+2\epsilon_B(\omega)}\right)\right] \times\left[1 - C_A\left(\frac{\epsilon_A(\omega)-\epsilon_B(\omega)}{\epsilon_A(\omega)+2\epsilon_B(\omega)}\right)\right]^{-1}\,. \tag{2.16}$$

On the other hand, if we make a self-consistent approximation by setting $\epsilon_0(\omega)=\epsilon(\omega)$, the effective medium approximation for $\epsilon(\omega)$ results.

$$\left\langle\frac{\epsilon_i(\omega)-\epsilon(\omega)}{\epsilon_i(\omega)+2\epsilon(\omega)}\right\rangle = 0\,. \tag{2.17}$$

In this case Eq. (2.11) simply reduces to

$$\vec{Q}(\vec{r})=\vec{E}_0(\vec{r})\,. \tag{2.18}$$

The formulation of the equation for Q as the first member of a hierarchy allows for the possibility of going beyond the EMT. For example, Hori and Yonezawa[38,39] have substantially improved the EMT for the DC conductivity by noting a formal analogy with the problem of an electron moving in a random medium and by exploiting higher-order cumulant approximations. A similar improvement could be introduced here.

In the case of a binary disordered medium Eq. (2.17) takes the form

$$C\left(\frac{\epsilon^0(\omega)-\epsilon(\omega)}{\epsilon^0(\omega)+2\epsilon(\omega)}\right)+(1-C)\left(\frac{\epsilon^1(\omega)-\epsilon(\omega)}{\epsilon^1(\omega)+2\epsilon(\omega)}\right)=0 \tag{2.19}$$

where

$$\epsilon^0(\omega)\equiv\epsilon(\omega),\quad C=1\,,$$
$$\epsilon^1(\omega)\equiv\epsilon(\omega),\quad C=0\,.$$

It is convenient to write the explicit solution of Eq. (2.19) in the following form:

$$\begin{aligned}&\epsilon(\omega)=\epsilon^0(\omega)f(x(\omega),C)\,,\\&f(x(\omega),C)=a(\omega)\pm[a(\omega)^2+\tfrac{1}{2}x(\omega)]^{1/2}\,,\\&a(\omega)=\tfrac{1}{2}\{(\tfrac{3}{2}C-\tfrac{1}{2})[1-x(\omega)]+\tfrac{1}{2}x(\omega)\}\,,\\&x(\omega)=\epsilon^1(\omega)/\epsilon^0(\omega)\,.\end{aligned} \tag{2.20}$$

The sign of the square root is chosen so as to give a solution with $\epsilon_2(\omega)\equiv\mathrm{Im}(\epsilon(\omega))\geqslant 0$. It is clear from the symmetry of Eq. (2.19) that the choice of C, ϵ^0, and ϵ^1 may be reversed without changing the results. This choice can therefore be guided by convenience. Finally, we note that the relationship between the frequency-dependent conductivity and $\epsilon_2(\omega)$ is $\sigma(\omega)=e_0\omega\epsilon_2(\omega)$, where $e_0=8.854\times10^{-12}$ and σ is in units of $(\Omega\,\mathrm{m})^{-1}$. If both components of the binary system possess a finite conductivity at $\omega\to0$, i.e., $\epsilon^1(\omega)$ and $\epsilon^0(\omega)$ increase as $1/\omega$ in this limit, Eq. (2.19) reduces to the well-known EMT equation for the dc conductivity.

In analogy with the EMT for the dc conductivity[19,20] a necessary condition for the validity of Eq. (2.17) for $0\leqslant C\leqslant 1$ is

$$0.05<|x(\omega)|<20\,. \tag{2.21}$$

When condition [Eq. (2.21)] is violated, the EMT does not yield correct results for concentration of component of higher absolute value of dielectric constant in the ranges $0.1<C<0.4$ since in this region percolation effects are important. In the case of a random medium with a continuous distribution function $P(\epsilon_i)$ a requirement analogous to Eq. (2.21) for the validity of EMT would be that the range of fluctuation in the local value of $\epsilon_i(\omega)$ is not too wide.

III. NUMERICAL SIMULATIONS OF THE COMPLEX DIELECTRIC CONSTANT

Numerical studies of the conductivity of a random network of resistors have proved important for the understanding of electronic transport in a random inhomogeneous medium.[19,20,22,23] A generalization of this approach for the case of frequency-dependent complex dielectric constant is presented herein. The random inhomogeneous medium with a correlation length b is viewed as divided into cells of dimension b. Each cell at r is assumed to be characterized by a real dielectric constant ϵ_r' and a conductivity σ_r. The following Maxwell equation is thus obeyed at r:

$$\vec{\nabla}\times\vec{H}(\vec{r})=\frac{\epsilon_r'}{C}\frac{\partial}{\partial t}\vec{E}(\vec{r})+\frac{4\pi}{C}\sigma_r\vec{E}(\vec{r})\,. \tag{3.1}$$

For a monochromatic wave of frequency ω

$$\vec{\nabla}\times\vec{H}(\vec{r})=-(i\omega/C)\epsilon_r(\omega)\vec{E}(\vec{r})\,, \tag{3.2}$$

where

$$\epsilon_r(\omega)=\epsilon_r'+i4\pi\sigma_r/\omega\,, \tag{3.2$'$}$$

and where ϵ_r' and σ_r can now be ω dependent. Operating with $\vec{\nabla}$ on Eq. (3.2) and bearing in mind that $\vec{\nabla}\cdot\vec{\nabla}\times\vec{H}=0$, we get

$$\vec{\nabla}\cdot[\epsilon_r(\omega)\vec{E}(\vec{r})]=0\,. \tag{3.3}$$

This equation serves as the basis for numerical simulation of the complex dielectric constant in analogy to the equation $\vec{\nabla}\cdot[\sigma_r\vec{E}(\vec{r})]=0$ for the simulation of dc conductivity.

The procedure of numerical simulation of $\epsilon(\omega)$ is based on the solution of Eq. (3.3) by a finite difference approximation. Introducing a cubic network of points $\vec{r}_i$ with spacing δ_r one obtains a system of linear equations.

$$\sum_j\epsilon_{ij}(\omega)(\phi_i-\phi_j)\;=0\,, \tag{3.4}$$

where the sum is over six neighbors of i

$$\epsilon_{ij}(\omega)=\delta r\epsilon^{(\omega)}_{\vec{r}=(\vec{r}_i+\vec{r}_j)/2} \tag{3.5}$$

and ϕ_i is the potential at $\vec{r}_i$. Each bond is assigned a value of ϵ according to the distribution function $P(\epsilon)$. For a binary system a fraction C of the bonds is assigned randomly the value ϵ^0, and the rest are assigned the value ϵ^1.

A simplified representation of the cubic network is shown in Fig. 1. The electromagnetic wave is assumed to be polarized in the x direction, and to propagate in the z direction. The network on which the numerical simulations are performed may be

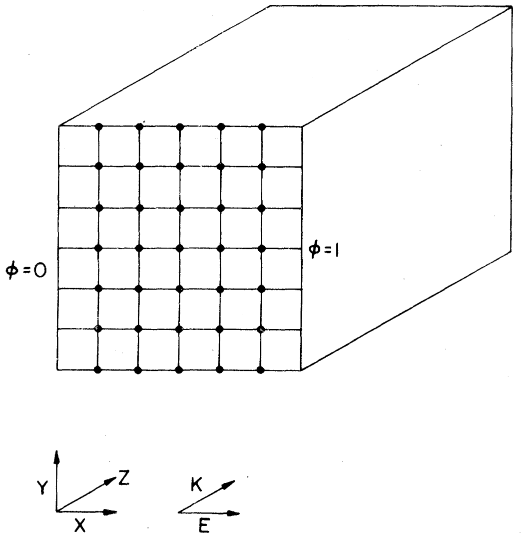

FIG. 1. Schematic description of the cubic network employed for the numerical simulation of the optical properties of a microscopically inhomogeneous medium.

considered to represent a cubic region of the medium small with respect to the wavelength but much larger than the average size of the correlation length for the fluctuations. Such a choice is possible since $\lambda \gg b$. The variation of the electric field over the sample due to the factor $e^{i\vec{k}\cdot\vec{r}}$ where $|k| = 2\pi/\lambda$ can therefore be disregarded so that the spatial dependence of the field amplitude will follow the fluctuations in the local complex dielectric constant $\epsilon_r(\omega)$. The system of N^3 equations [Eq. (2.4)] is solved by means of an over-relaxed Gauss-Seidel iteration procedure with the following boundary conditions: (i) constant potentials $\phi = 0$ on the $x = 0$ face of the cube and $\phi = 1$ on the opposite face; (ii) cyclic boundary conditions in the y and z directions. The initial potential values for the iterations are linear in the x direction and constant over the yz planes. The average value of the complex displacement in the slab formed by the n and $(n+1)$ yz planes is evaluated by

$$D_{n,n+1} = \frac{1}{N_{yz}} \sum_{k,k'} \epsilon_{kk'} \frac{\phi_k - \phi_{k'}}{\delta r} , \qquad (3.6)$$

where k and k' represent neighboring sites on the two planes, ϕ_k, $\phi_{k'}$ are the (complex) potentials that solve Eq. (3.4), and N_{yz} is the number of sites in yz planes. The direction of $D_{n,n+1}$ is parallel to the field imposed on the cube, and normal to the yz planes. The continuity of the normal component of $\vec{D}$ across surfaces implies the equality

$$D_{1,2} = D_{2,3} = \cdots = D_{N-1,N} . \qquad (3.7)$$

This is also the final value of D. Finally, the effective dielectric constant $\epsilon(\omega)$ of a random medium is defined by the relation

$$\epsilon(\omega)\langle E\rangle = \langle D\rangle = \langle \epsilon_r(\omega) E_r\rangle , \qquad (3.8)$$

where ϵ_r and E_r are the local values of the dielectric constant and the field. In this case $\langle E\rangle = 1/L$ so that ϵ is given by $\epsilon = DL$.

In simulating the dielectric properties of a binary material one deals with a continuous percolation problem.[15-18] The random cubic network simulation described above, which is an extension of Kirkpatrick's model for the dc conductivity,[19] is related however to bond percolation on a sc lattice. We have shown recently[20] that a closer simulation of a continuous system can be obtained by imposing correlations between the ϵ values assigned to neighboring bonds. Regions of $\epsilon = \epsilon^1$ or of $\epsilon = \epsilon^0$ are formed which extend over several lattice distances. The effect of correlation is mainly to shift the percolation threshold from $C^* = 0.25$ to $C^* \cong 0.15 \pm 0.01$ which corresponds to the threshold in a random continuous system. Numerical simulations for model systems demonstrate that this effect is evident only when $|\epsilon^1/\epsilon^0| < 0.05$. Otherwise

$$\epsilon(\omega)^{\text{EMT}} \simeq \epsilon(\omega)^{\text{non cor}}_{\text{num}} \simeq \epsilon(\omega)^{\text{cor}}_{\text{num}}$$

throughout the entire concentration range.

IV. APPLICATIONS TO SOME MODEL SYSTEMS

In this section we apply the effective-medium theory together with numerical network simulations of $\epsilon(\omega)$ to explore the optical and microwave properties of some simple inhomogeneous model systems. These results will enable us to gain some insight into the gross features of the optical constants and the frequency-dependent conductivity of microscopically inhomogeneous materials. We shall be able to establish the criteria for the validity of the EMT and of the Maxwell-Garnett relation on the basis of direct comparison with numerical results. We shall start our discussion by considering a binary metal-insulator inhomogeneous system, which is relevant to the understanding of the optical properties of granular metals.[1-4] Another system studied by us involves again a binary metal-nonmetal mixture where the nonmetallic regimes are characterized by a Lorentz-type dielectric constant centered around a frequency ω_0 which is lower than the plasma frequency ω_p of the metallic regions. Such a model is of interest for understanding the optical properties of inhomogeneous materials undergoing a metal-nonmetal transition, such as metal-ammonia solutions.[31] Next, we focus attention on the dielectric function of a dielectric material containing voids, which is pertinent to the elucidation of the optical properties of amorphous germanium.

A. Drude metal-insulator system

We consider a binary disordered medium where the metallic regions are characterized by a Drude dielectric function

$$\epsilon^0(\omega) = 1 - \omega_p^2/\omega(\omega + i\gamma)\,, \qquad (4.1)$$

where ω_p is the plasma frequency and γ is the inverse relaxation time, while for the insulating region we take

$$\epsilon^1(\omega) = \epsilon^1\,, \qquad (4.2)$$

where ϵ^1 is real and frequency independent.

We now proceed to the study of Mie resonances exhibited by metallic particles embedded in a dielectric.[1-7] In Fig. 2 we display the results of numerical simulations of the optical properties of a two-component system where the optical properties of the metallic regions of volume fraction C are given by Eq. (4.1) with $\gamma/\omega_p = 0.4$ while the nonmetallic regions of volume fraction $1 - C$ are characterized by Eq. (4.2) with $\epsilon^1 = 1$. These numerical data for $0 < C < 0.25$ are compared with predictions of the EMT, Eq. (2.17), and of the Maxwell-Garnett (MG) relation, Eq. (2.16). Below the percolation threshold $C^* = 0.15 \pm 0.01$ there is good agreement between the results of the EMT and the numerical simulations, as is evident for the data for $C = 0.046$, 0.1, 0.15, and 0.25 in Figs. 2(a)–2(d), respectively. At $C = 0.25$ the numerical

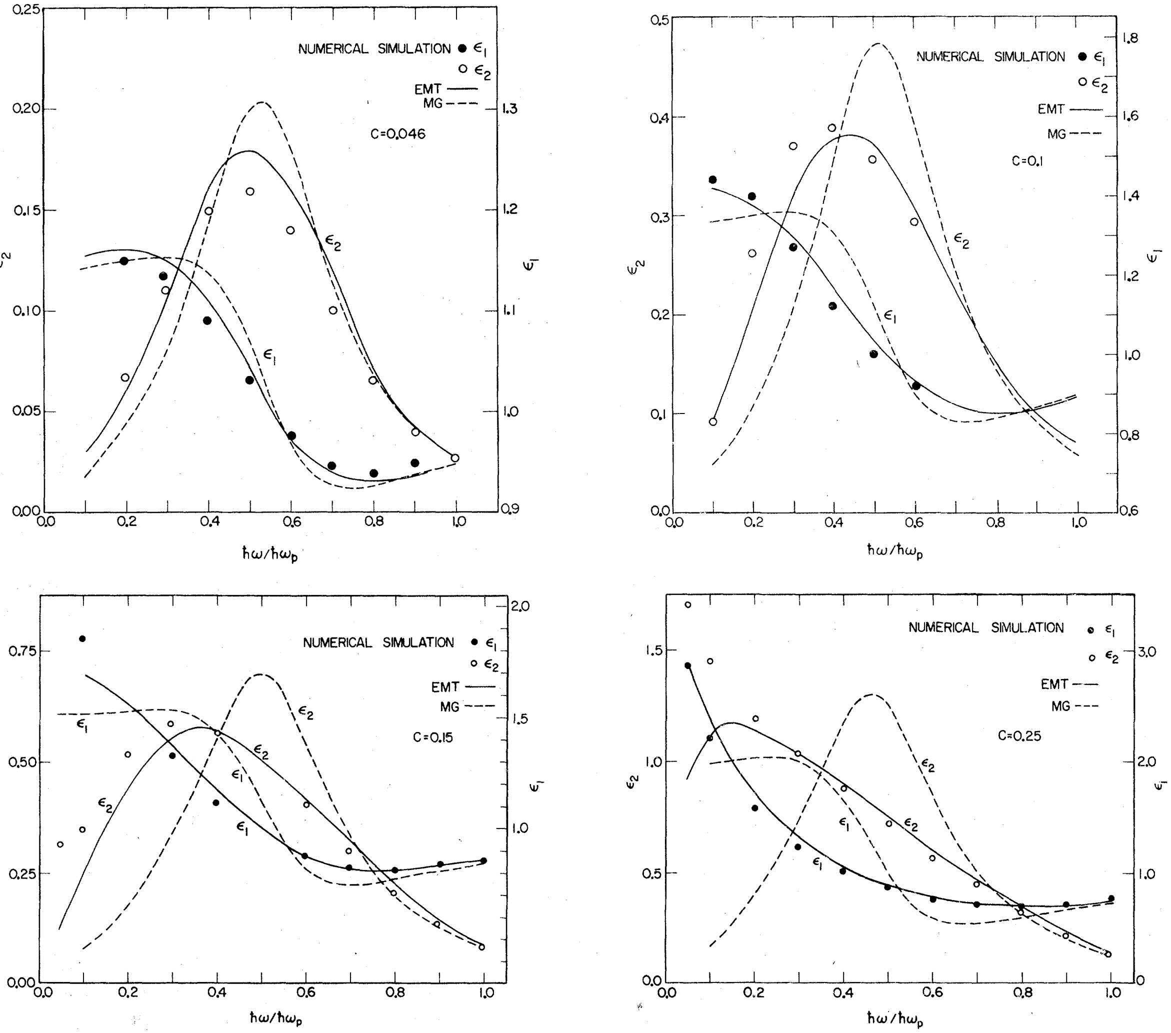

FIG. 2. Complex dielectric function of a Drude metal-insulator two-component inhomogeneous system evaluated by numerical simulation, effective medium theory (EMT) and the Maxwell-Garnett (MG) relation. The dielectric function $\epsilon^0(\omega)$ of the metallic regions (with probability C) is given by Eq. (4.1) with $\gamma/\omega_p = 0.4$, while for the nonmetallic regions (with probability $1 - C$) $\epsilon^1 = 1$.

results exhibit a fast increase of $\epsilon_2(\omega)$ as $\omega \to 0$, while the EMT still predicts a broad peak at finite ω. The same broad peak for $C = 0.25$ is observed in the results calculated on the basis of the Maxwell-Garnett relation. This discrepancy between the EMT and the MG schemes, Eqs. (2.17) and (2.16), and the results of the numerical simulations originates from the failure of the mean-field theories above the percolation threshold. The apparent percolation threshold in the EMT is $C^*_{\text{EMT}} = 0.33$ which is considerably higher than the value $C^* = 0.15 \pm 0.02$ characterizing a random continuous system. Figure 2(d) reveals that the disagreement between $\epsilon(\omega)$ obtained from the EMT and from numerical simulations occur when $|x(\omega)| < 0.05$, in agreement with the general criteria for the validity of the EMT presented in Sec. III. The EMT fails at $\omega < \gamma$ where $|\epsilon^0(\omega)|$ assumes high values. We thus conclude that Mie resonances characterized by a maximum in $\epsilon_2(\omega)$ are exhibited in a binary metal-insulator random mixture in the range $0 < C < C^*$. For $C > C^*$, $\epsilon_2(\omega)$ assumes a metallic-type behavior, reflecting the effect of the metal-nonmetal transition on the optical properties.

Experimental results[6] on metallic films show Mie resonance peaks for $C = 0.1-0.2$. Some recent data on granular metals show a persistence of the peaks up to 60% metal without any comparable shift to the red.[4] It is, however, apparent from the conductivity data, which show a transition to metallic behavior at $C = 0.4-0.6$ instead of the value $C^* = 0.15-0.2$ expected for a random inhomogeneous system, and from the structure revealed by electron micrograph of metallic regions isolated from one another by an insulating matrix which persists up to $C = 0.5$, that the Ag-SiO_2 and Au-SiO_2 films are not random to the degree required for the validity of our theory. The optical data for granular metals were treated[4] by the application of the MG theory. The basic assumption underlying the MG theory, that of metal regions isolated by an insulating matrix, holds up to about $C = 0.5$ for these materials. The only approximation which might be inaccurate is the use only of dipolar fields. One expects, therefore the MG theory to hold better for granular metals than the EMT, and indeed it does, as can be seen from the comparison between the two schemes given in the Appendix.

B. Drude-metal-Lorentzian resonance

The Li-NH_3 and Na-NH_3 in the range of metallic concentration 2.3–9 MPM consist of metallic and nonmetallic regions characterized by a Debye short correlation length of 15–30 Å.[22] The optical properties of the metallic component $\epsilon^0(\omega)$ are described quite well by the Drude model[29-31] with $\omega_p \sim 1.6-1.9$ eV and $\gamma \approx 0.4-0.5$ eV. The nonmetallic component exhibits a wide peak in $\epsilon_2^1(\omega)$ centered at ~0.65 eV, which corresponds to the red-shifted absorption peak of the electron cavity resonance observed at lower metal concentration. In order to mimic the gross features of the optical properties of metal-ammonia solutions in the inhomogeneous regime, we have performed numerical simulation of $\epsilon(\omega)$ for a model system where $\epsilon^0(\omega)$ of the metallic regions is given by the Drude form, Eq. (4.1), while the nonmetallic regions are characterized by the Lorentz function

$$\epsilon^1(\omega) = 1 - f/(\omega^2 - \omega_0^2 + i\gamma_L\omega) , \qquad (4.3)$$

where the resonance is characterized by a peak at the energy ω_0, a width γ_L and an oscillator strength f. In Fig. 3, we present the numerical results together with the predictions of the EMT and the MG equation. For $\omega > 0.1\omega_p$, where $|x(\omega)|$ is of the order of unity, the agreement between the numerical results and the EMT is excellent, as expected. On the other hand, the MG relation is inapplicable, as it is unjustified to approximate the zero-order value of $\epsilon(\omega)$. We conclude that for such systems the resonance structure of the Lorentzian characterizing the nonmetallic regions persists for high values of C. Even for $C \simeq 0.8$ a pronounced peak in $\epsilon_2(\omega)$ and an inflection in $\epsilon_1(\omega)$ are exhibited. A detailed analysis of the optical properties of metal-ammonia solutions demonstrates the persistence of the resonance structure at high metal concentrations, in accord with the results of the present model calculations.

C. Lorentzian-void resonance

Our theory is applicable to the study of the effects of submicroscopic voids in a semiconducting medium which is characterized by a Lorentzian dielectric function. Amorphous films of Ge and Si contain voids which are assumed to account for their (10–30)% density deficit with respect to the crystalline substances.[40-42] The form, size, and volume fraction of the voids was found to vary widely with the deposition method and with the substrate temperature.[43-46] In recent small angle x-ray scattering experiments Schevchik and Paul[46] found that a-Ge films prepared by evaporation contain about 10% of approximately spherical voids with size distribution peaked at $b \sim 15$ Å. Sputtered films contained ~10% of smaller voids with $b \lesssim 5$ Å. Galeener[9] has interpreted the observed void resonance by means of a MG formula for nonspherical voids. He assumed that the voids are disklike with normals lying on the surface of the films. There is no evidence that this type of void struc-

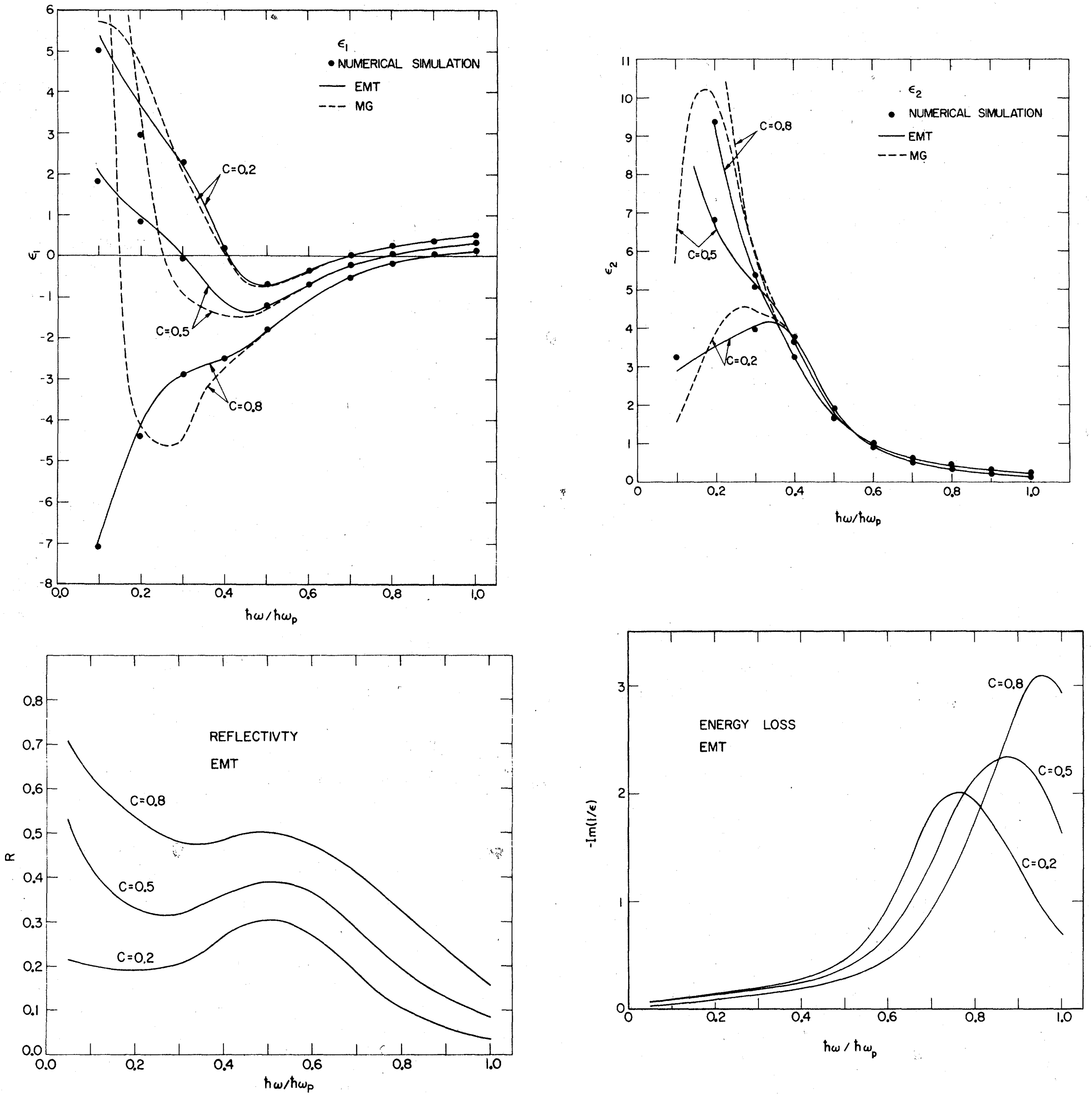

FIG. 3. Optical properties of a two-component inhomogeneous system where the dielectric function $\epsilon^0(\omega)$ of the metallic regions is given by the Drude model dielectric function [Eq. (4.1)] with $\gamma/\omega_p = 0.25$, while the nonmetallic regions are characterized by a Lorentz function [Eq. (4.3)] with $\gamma_L/\omega_p = 0.25$, $\omega_0/\omega_p = 0.4$, and $f = 0.36$. (a) $\epsilon_1(\omega)$; (b) $\epsilon_2(\omega)$; (c) EMT reflectivity; (d) EMT energy-loss function.

ture is a general feature of the a-Ge films,[46] and we shall show that the gross features of the optical spectra are well represented in terms of our theory. We have calculated $\epsilon(\omega)$ by the EMT for volume fractions of voids $C = 0.06$ and $C = 0.12$. In these calculations $\epsilon^1 = 1$ (the void component) and

$$\epsilon^0(\omega) = 1 - A/(\omega^2 - \omega_0^2 + i\gamma\omega) , \qquad (4.4)$$

with $\gamma = 0.4$ eV, $\hbar\omega_0 = 3$ eV, and $A = 250$. With these dielectric functions for $\epsilon^0(\omega)$ and $\epsilon^1(\omega)$ the validity condition for the EMT is well obeyed. The parameters characterizing $\epsilon^0(\omega)$ were chosen to agree roughly with the characteristics of the absorption peak observed in a-Ge films.[10,11] The main effect of the voids on $\epsilon_2(\omega)$ is a reduction in the peak height of ~10 and 20% for $C = 0.06$ and $C = 0.12$, respectively (Fig. 4). A comparison of the peak height of $\epsilon_2(\omega)$ between two sputtered a-Ge films

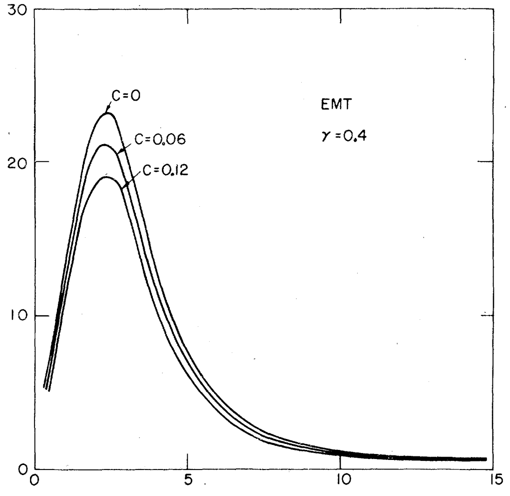

FIG. 4. Results of EMT calculations of $\epsilon_2(\omega)$ for a medium characterized by a Lorentzian dielectric function $\epsilon^0(\omega)$ given by [Eq. (4.4)] with $\gamma = 0.4$ eV, $\hbar\omega_0 = 3$ eV, and $A = 250$, containing a volume fraction C of voids with $\epsilon^1 = 1$.

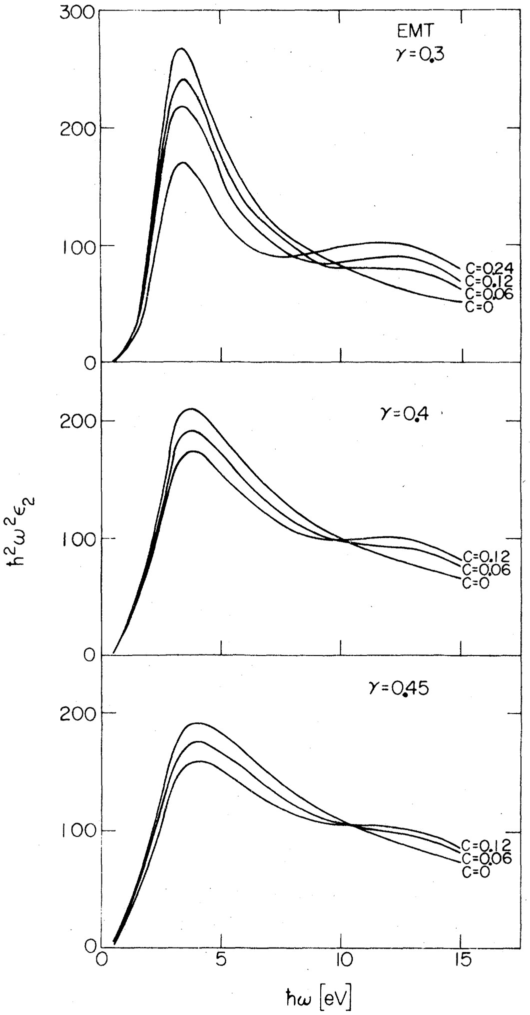

FIG. 5. Optical transition strength $(\hbar\omega)^2\epsilon_2(\omega)$ evaluated by EMT for a Lorentzian medium with voids. $\epsilon^0(\omega)$ and ϵ^1 are identical with these for Fig. 4 with $\gamma = 0.3$, 0.4, 0.45.

grown at $T_s = 350\,^\circ$C and at $T_s = 25\,^\circ$C shows[45] a decrease of ~10% for the film characterized by the lower value of T_s. The films sputtered at high T_s are close in density to crystalline Ge, and can be considered voidless. A decrease of ~17% in the peaks height was observed by Bauer *et al.*[10] as T_s decreased from 160 to 22 °C. These effects, together with the estimates of ~10% volume fraction of voids are consistent with the present theoretical result. Another feature observed in the experimental $\omega^2\epsilon_2(\omega)$ spectrum, is a broad shoulder at 8–12 eV.[10,11] A wide resonance similar to that observed in the experiment appears in $\epsilon(\omega)$ (Fig. 5). In the absence of complete data on the voidless phase a quantitative comparison is not possible. A comparison between the void resonance evaluated by the MG formula with that of the EMT is presented in Fig. 6.

V. ac AND MICROWAVE PROPERTIES OF $\epsilon(\omega)$

We now examine the frequency-dependent behavior of the complex dielectric constant and the conductivity of binary metal-insulator mixtures at microwave frequencies. Within this range

$$\epsilon^0(\omega) = \epsilon_1^0 + i\sigma^0/e_0\omega\,, \quad \omega \ll \frac{\sigma^0}{e_0}\,, \quad |\epsilon^0(\omega)| \gg 1\,. \tag{5.1}$$

Since $\epsilon^1(\omega)$ is the complex dielectric constant of a nonmetal we also have

$$|x(\omega)| = |\epsilon^1(\omega)/\epsilon^0(\omega)| \ll 1\,. \tag{5.2}$$

Under the condition Eq. (5.2), the EMT result for $\epsilon(\omega)$ reduces to

$$\epsilon(\omega) = \epsilon^0(\omega)(\tfrac{3}{2}C - \tfrac{1}{2}) \tag{5.3}$$

in the region $C > C^*_{\mathrm{EMT}} \cong 0.33$.

Numerical simulations of $\epsilon(\omega)$ reproduce the result Eq. (5.3) for $C > 0.4$. We may conclude that in a random binary system the metallic character of $\epsilon(\omega)$ is preserved down to metallic volume fractions of $C = 0.4$.

Below the percolation threshold, EMT yields

$$\epsilon(\omega) = \epsilon^1(\omega)/(1 - C/C^*_{\mathrm{EMT}})\,, \quad C < 0.2\,, \quad C^*_{\mathrm{EMT}} = \tfrac{1}{3}\,. \tag{5.4}$$

If $\epsilon_2^1(\omega) < \epsilon_1^1(\omega)$, it is necessary to go over to a higher-order expansion in the small parameter $|x(\omega)|$ in order to obtain the correct ω dependence of $\epsilon_2(\omega)$

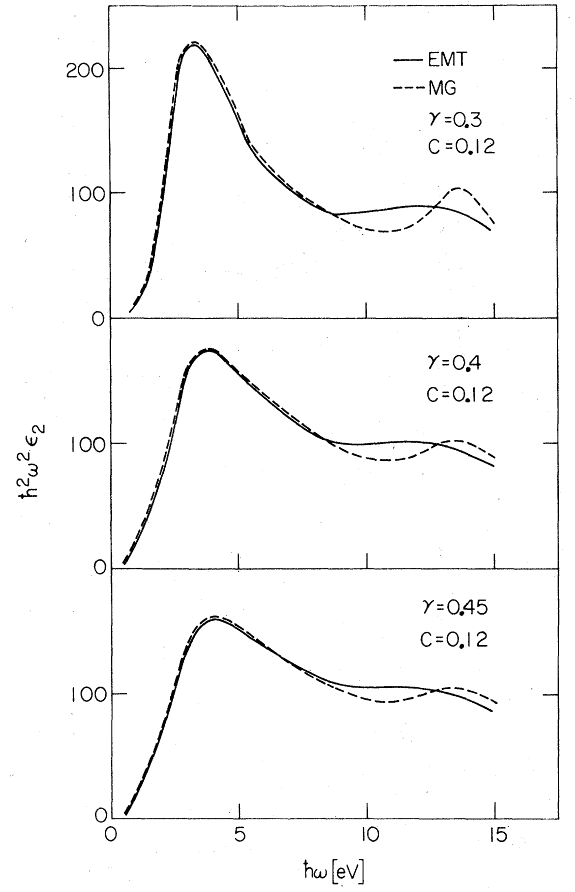

FIG. 6. Optical transition strength $(\hbar\omega)^2\epsilon_2(\omega)$ evaluated by EMT and MG theory. $\epsilon^0(\omega)$ and ϵ^1 are identical with these for Fig. 4.

$$\epsilon_2(\omega)=\frac{\epsilon_2^1(\omega)}{1-C/C^*_{\rm EMT}}+\frac{e_0(\omega)\times 9(1-C)C}{\sigma^0(1-C/C^*_{\rm EMT})^3}\{[\epsilon_1^1(\omega)]^2+[\epsilon_2^1(\omega)]^2\}, \quad (5.5)$$

$$\sigma(\omega)=e_0\epsilon_2(\omega)\omega .$$

The second term in Eq. (5.5) is dominant if the following inequality is obeyed:

$$\epsilon_2^1<9C(\epsilon_1^1)^2e_0(\omega)/\sigma^0 . \quad (5.6)$$

For a dielectric $\epsilon_1^1(\omega)>\epsilon_2^1(\omega)$ usually holds, and $\epsilon_1^1(\omega)$ is a slowly varying function of ω. Under the condition Eq. (5.6) or in the limiting case of $\epsilon_2^1=0$ we thus have $\sigma(\omega)\propto\omega^2$ for low concentrations of the metallic component.

At the transition region $C\sim C^*_{\rm EMT}$ for frequencies which obey $|x(\omega)|\ll 1$ we have from Eq. (2.16)

$$\epsilon(\omega)=[\tfrac{1}{2}\epsilon^0(\omega)\epsilon^1(\omega)]^{1/2} . \quad (5.7)$$

Since $|\epsilon^0(\omega)|\propto 1/\omega$ and $|\epsilon^1(\omega)|$ is weakly frequency dependent Eq. (5.7) yields

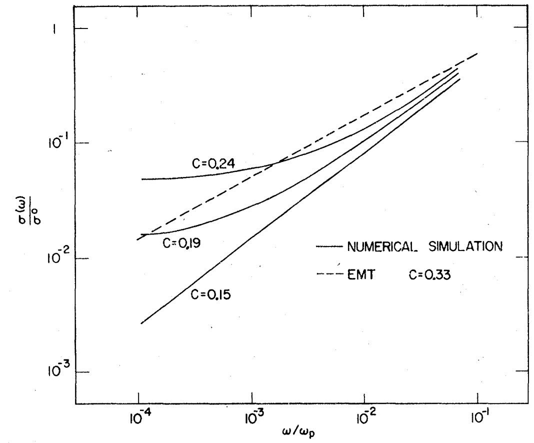

FIG. 7. Results of numerical simulation for the frequency-dependent conductivity of a metal-nonmetal inhomogeneous medium at metallic volume fractions C near C^*. $\epsilon^0(\omega)$ is given by the Drude model dielectric function with $\gamma=\frac{1}{6}$ and $\omega_P=1$ while $\epsilon^1=40+20i$. $\sigma^0\equiv\sigma(\omega=0,C=1)$. (Straight line) numerical simulation on bond correlated networks; (dashed line) EMT, $C=0.33$.

$$\epsilon(\omega)\propto\omega^{-0.5} , \quad \sigma(\omega)\propto\omega^{0.5} . \quad (5.8)$$

If $\epsilon^1(\omega)=\epsilon^1$ is real and frequency independent, we have

$$\sigma(\omega)=(\tfrac{1}{2}\epsilon_1 l_0 e_0\sigma^0)^{1/2}\omega^{0.5} . \quad (5.9)$$

Numerical simulations at $C\sim C^*$ result in a similar frequency-dependent behavior, $\sigma(\omega)\propto\omega^s$. The exponent s depends on C and varies from $s=0.75$ for $C\lesssim C^*$ to $s=0.5$ for $C=C^*$. Numerical results for $C\simeq C^*$ are presented together with $\epsilon_{\rm EMT}(\omega)$ at $C\simeq 0.33$ in Fig. 7.

We now compare these general conclusions with some ac conductivity data. In annealed granular metal films[47,48] the transition to metallic behavior occurs at metallic volume fraction $C\simeq 0.47\pm 0.05$, while for a three-dimensional random system the percolation threshold $C^*\simeq 0.145\pm 0.005$. The reason for this discrepancy is that in the annealed films the grains have grown so that the metal regions are isolated by an insulating matrix up to $C\simeq 0.45$–0.47,[49] as indicated by electron micrography and the persistence of the Mie resonance (Sec. IV A). The conduction is then by a (three dimensional) percolation process for which $C^*\simeq 0.5$. The application of our present random medium models to these systems is still meaningful if we compare experimental data in the nonmetallic regime $C<C^*$. Similarly, the metallic regime $C>C^*$ should be compared with the theory for $C>C^*$:

(a) $C>C^*$—EMT and numerical simultions predict a decrease of $\sigma(\omega)$ with decreasing C according to Eq. (5.3). Since in the ac and microwave regions $\omega\ll\gamma,\omega_p$, no change of the ω-dependent behavior of $\sigma(\omega)$ from the metallic behavior is expected. The reported[47,48] experimental data for metallic $\sigma(\omega)$ show an increased skin depth as C decreases in agreement with the theory.

(b) $C<C^*$—According to the EMT result for a metal-dielectric system, Eq. (5.5), $\sigma(\omega)$ follows the frequency-dependent conductivity of the dielectric matrix at low ω values. At higher frequencies the second term in Eq. (5.5) becomes dominant, and $\sigma(\omega)\propto\omega^2$ is predicted.

The ac conductivity of granular films in the nonmetallic regime at low ($\omega<6\times10^6$ sec^{-1}) frequencies manifests a $\sigma\propto\omega^s$ dependence with $s\sim0.8$.[50,51] The ω-dependent term in the conductivity of the dielectric matrix of these films Al_2O_3, SiO_2, and SnO_2 follow a similar power law[52] in the same low-frequency range ($\omega<6\times10^6$). We can attribute the ω^s behavior of these granular films to the ac transport properties of the dielectric. For higher frequencies ($\omega=6\times10^8$ sec^{-1}), Abeles *et al.*[47] report a $\sigma(\omega)\propto\omega^2$ behavior in granular films in the nonmetallic regime. At this higher-frequency range the second term in Eq. (5.5) becomes dominant.

An increase of $\epsilon_1(\omega)$ with increasing C has been observed in granular films in the nonmetallic regime. The value of $\epsilon_1(\omega)$ increased up to ~100 as the percolation threshold was approached. Such behavior of the dielectric constant is predicted by EMT, as evident from Eq. (5.4). A similar effect has been observed in the microwave region in Na-NH_3 solutions.[31,53]

APPENDIX: RESONANCE OF $\epsilon(\omega)$ IN A METAL-INSULATOR SYSTEM WITHIN THE MG AND EMT SCHEMES

The complex dielectric constant $\epsilon(\omega)$ of a binary metal insulator system is given according to the MG theory by

$$\epsilon(\omega)=\epsilon^1(\omega)[1+2K(\omega)]/[1-K(\omega)]\,, \tag{A1a}$$

where

$$K(\omega)=C[\epsilon^0(\omega)-\epsilon^1(\omega)]/[\epsilon^0(\omega)+2\epsilon^1(\omega)]\,, \tag{A1b}$$

and where C is the concentration of the metallic compound $\epsilon^0(\omega)$ embedded in a medium of dielectric constant $\epsilon^1(\omega)$.

The resonances of $\epsilon(\omega)$ given by Eq. (A1a), occur at energies $h\omega_R$ for which the following condition is obeyed:

$$\mathrm{Re}[K(\omega)-1]=0\,. \tag{A2}$$

Equation (A2) may be transformed into

$$\mathrm{Re}[(2+C)\epsilon^1(\omega)+(1-C)\epsilon^0(\omega)]=0\,. \tag{A3}$$

We specialize now to the model system which consists of a Drude metal and a perfect insulator characterized by

$$\epsilon^0(\omega)=1-\omega_P^2/\omega(\omega+i\gamma)\,, \tag{A4a}$$

$$\epsilon^1(\omega)=\epsilon^1\,. \tag{A4b}$$

For small C values ($C<\gamma/\omega_P$)

$$\omega_R\cong\omega_P/(2\epsilon^1+1)^{1/2}\,. \tag{A5}$$

The half width of the resonance is given by

$$\Delta\omega_R=\gamma\,, \tag{A6}$$

and the peak height is linear in C

$$\epsilon_2(\omega_R)=(2\epsilon^1+1)^{1/2}(\omega_P/\gamma)C\,. \tag{A7}$$

The EMT formula for $\epsilon(\omega)$ may be recast in the following form:

$$\epsilon(\omega)=\frac{\epsilon^1(1+L(\omega))+\epsilon(\omega)L(\omega)}{1-L(\omega)}\,, \tag{A8a}$$

$$L(\omega)=\frac{C}{1-C}\,\frac{\epsilon^0(\omega)-\epsilon(\omega)}{\epsilon^0(\omega)+2\epsilon(\omega)}\,. \tag{A8b}$$

For small C values setting $\epsilon(\omega)\sim\epsilon^1(\omega)$ and $1-C\sim1$ in the right-hand side of Eqs. (A8a) and (A8b) leads to the MG formula Eq. (A1). This qualitative observation will be studied now in more detail near $\omega=\omega_R$. For $C<\gamma/\omega_P$ Eq. (A1) may be approximated by

$$\epsilon(\omega)=\epsilon^1[1+3K(\omega)]\,. \tag{A9}$$

The resonance frequency is now given by the pole of $K(\omega)$ and is thus determined by the condition

$$\mathrm{Re}[2\epsilon^1+\epsilon_0(\omega)]=0\,. \tag{A10}$$

The EMT expression Eq. (A8) may also be reduced by a small C expansion to Eq. (A9). The criterion for the validity of this approximation may be obtained by handling the explicit expression for $\epsilon^{\mathrm{EMT}}_{(\omega)}$, Eq. (2.20). The following condition on C has to hold:

$$\left|\frac{[2\epsilon^1-\epsilon^0(\omega)][\epsilon^0(\omega)-\epsilon^1]}{[2\epsilon^1+\epsilon^0(\omega)]^2}\right|C\ll1\,. \tag{A11}$$

For the Drude metal-insulator system with $\epsilon^0(\omega)$ given by Eq. (A4a) and $\epsilon_1^1=1$, Eq. (A11) reduces at $\omega=\omega_R=\omega_{P/3}$ to the following condition:

$$C\ll\gamma^2/2\omega_P^2\,. \tag{A12}$$

At C values given by Eq. (A12) $\epsilon^{\mathrm{EMT}}_{(\omega)}$ reproduces the narrow resonance of the MG model. At higher metal concentration the peak in $\epsilon^{\mathrm{EMT}}_{(\omega)}$ broadens and is shifted to lower frequencies as C increases towards C^*. At $C>C^*_{\mathrm{EMT}}=0.33$ $\epsilon^{\mathrm{EMT}}_{(\omega)}$ has a maximum at $\omega=0$, and is qualitatively similar to $\epsilon^0(\omega)$. In the MG scheme which represents a set of isolated metallic regions embedded in a matrix characterized by $\epsilon=\epsilon_1^1$, $\omega_R(C)$ as given by solving Eq. (A3) decreases slowly with increasing C and approaches zero as $C\to1$. The MG resonance width does not increase significantly with increasing metal concentration.

*Research supported by the U.S.-Israel Binational Science Foundation at Tel-Aviv University and by the L. Block Fund, NSF Grant No. DMR75-13343 and the Materials Research Laboratory of the NSF at The University of Chicago.

[1] O. S. Heavens, *Optical Properties of Thin Solid Films* (Dover, New York, 1965).

[2] W. Hampe, Z. Phys. 152, 470 (1958); 152, 476 (1958).

[3] G. Rasigni and D. Rouard, J. Opt. Soc. Am. 53, 604 (1963).

[4] R. W. Cohen, G. D. Cody, M. D. Coutts, and B. Abeles, Phys. Rev. B 8, 3689 (1973).

[5] M. Faraday, Philos. Trans. R. Soc. Lond. A 147, 145 (1857).

[6] E. H. Doremus, J. Chem. Phys. 40, 2389 (1964); J. Appl. Phys. 37, 2775 (1966); J. Chem. Phys. 42, 414 (1965).

[7] U. Kreibig and C. V. Fragstein, Z. Phys. 224, 307 (1969).

[8] W. Doyle, Phys. Rev. Lett. 111, 1067 (1958).

[9] F. L. Galeener, Phys. Rev. 27, 421 (1971); Phys. Rev. Lett. 27, 1716 (1971).

[10] R. S. Bauer, F. L. Galeener, and W. E. Spicer, J. Non-Cryst. Solids 8-10, 196 (1972).

[11] T. M. Donovan, W. E. Spicer, J. M. Bennet, and E. J. Ashley, Phys. Rev. B 2, 397 (1970).

[12] G. Mie, Ann. Phys. 25, 377 (1908).

[13] J. C. Maxwell-Garnett, Philos. Trans. R. Soc. Lond. 203, 385 (1906).

[14] J. P. Marton and J. R. Lemon, Phys. Rev. B 4, 271 (1971).

[15] V. K. S. Shante and S. Kirkpatrick, Adv. Phys. 20, 235 (1971).

[16] M. H. Cohen, in *Electrons in Fluids*, edited by J. Jortner and N. R. Kestner (Springer, Berlin, 1973).

[17] R. Zallen and R. Scher, Phys. Rev. B 4, 4771 (1971).

[18] H. Scher and R. Zallen, J. Chem. Phys. 53, 3759 (1970).

[19] (a) S. Kirkpatrick, Phys. Rev. Lett. 27, 1722 (1971). (b) S. Kirkpatrick, Rev. Mod. Phys. 45, 574 (1973).

[20] (a) I. Webman, J. Jortner, and M. H. Cohen, Phys. Rev. B 11, 2885 (1975). (b) I. Webman, J. Jortner, and M. H. Cohen (unpublished).

[21] A. S. Skal, B. I. Shklovskii, and A. L. Efros, JETP Lett. 17, 552 (1973).

[22] (a) J. Jortner and M. H. Cohen, J. Chem. Phys. 58, 5170 (1973). (b) J. Jortner and M. H. Cohen, Phys. Rev. B 13, 1548 (1976).

[23] I. Webman, M. H. Cohen, and J. Jortner, Phys. Rev. B 13, 713 (1976).

[24] D. A. G. Bruggeman, Ann. Phys. (Leipz.) 24, 636 (1935).

[25] R. Landauer, J. Appl. Phys. 23, 779 (1952).

[26] M. H. Cohen and J. Jortner, Phys. Rev. Lett. 30, 696 (1973).

[27] M. H. Cohen and J. Jortner, Phys. Rev. A 10, 778 (1974).

[28] (a) M. H. Cohen and J. Jortner, in *Proceedings of the Fifth International Conference on Amorphous and Liquid Semiconductors, Garmisch*, edited by J. Stuke and W. Brenig (Taylor and Francis, London, 1974), p. 167. (b) M. H. Cohen and J. Jortner, J. Phys. (Paris) 35, C4-345 (1974).

[29] W. T. Cronenwett and J. C. Thompson, Adv. Phys. 16, 439 (1967).

[30] R. B. Somoano and J. C. Thompson, Phys. Rev. A 1, 376 (1970).

[31] M. H. Cohen, I. Webman, and J. Jortner, J. Chem. Phys. 64, 2013 (1976).

[32] Z. Hashin and S. A. Shtrikman, J. Mech. Phys. Solids 11, 127 (1963).

[33] B. E. Springett, Phys. Rev. Lett. 31, 1463 (1973).

[34] M. Born and E. Wolf, *Principles of Optics* (Pergamon, New York, 1965).

[35] M. Lax, Rev. Mod. Phys. 23, 287 (1951).

[36] M. Lax, Phys. Rev. 85, 621 (1952).

[37] (a) H. A. Lorentz, Wiedem. Ann. 9, 641 (1880). (b) L. Lorenz, *ibid.* 11, 170 (1881).

[38] M. Hori and F. Yonezawa, J. Math. Phys. 16, 352 (1975).

[39] D. Stroud, Phys. Rev. B 12, 3368 (1975).

[40] H. Ehrenreich and D. Turnbull, Comments Solid State Phys. 3, 75 (1970).

[41] A. H. Clark, Phys. Rev. 154, 750 (1967).

[42] T. M. Donovan, E. J. Ashley, and W. E. Spicer, Phys. Lett. A 32, 85 (1970).

[43] T. M. Donovan and K. Heinemann, Phys. Rev. Lett. 27, 1794 (1971).

[44] G. S. Cargyll, III, Phys. Rev. Lett. 28, 1372 (1972).

[45] R. J. Temkin, G. A. N. Connell, and W. Paul, in *Proceedings of the Fifth International Conference on Amorphous and Liquid Semiconductors, Garmisch*, edited by J. Stuke and W. Brenig (Taylor and Francis, London, 1974), p. 533.

[46] N. J. Shevchik and W. Paul, J. Non-Cryst. Solids 16, 55 (1974).

[47] B. Abeles, Ping Sheng, M. D. Coutts, and Y. Arie, Adv. Phys. 24, 407 (1975).

[48] B. Abeles, H. L. Pinch, and J. J. Gittleman, Phys. Rev. Lett. 35, 247 (1975).

[49] M. H. Cohen, I. Webman, and J. Jortner (unpublished).

[50] J. J. Hauser, Phys. Rev. 137, 4099 (1973).

[51] P. A. Tick and F. P. Fehlner, J. Appl. Phys. 43, 362 (1972).

[52] (a) A. K. Jonscher, in *Electrons and Structural Properties of Amorphous Semiconductors*, edited by P. G. Le Comber and J. Mort (Academic, New York, 1973), p. 329. (b) A. K. Jonscher, J. Phys. C 6, L235 (1973).

[53] D. W. Mahaffey and D. A. Jerde, Rev. Mod. Phys. 40, 710 (1968).